Manufacture of syntactic foams: pre-mold processing

Md Mainul Islam and Ho Sung Kim [1]

Discipline of Mechanical Engineering

School of Engineering

Faculty of Engineering and Built Environment

The University of Newcastle

Callaghan, NSW 2308

Australia

Phone +61 2 4921 6211 Fax +61 2 4921 6946

Email: ho-sung.kim@newcastle.edu.au

Abstract

Manufacturing process for syntactic foams made of hollow microspheres and starch was studied. Various manufacturing parameters in relation with the 'buoyancy method' were identified and inter-related. An equation based on unit cell models with the minimum inter-microsphere distance (MID) concept for a relation between volume expansion rate (VER) of bulk microspheres in aqueous starch and microsphere size was derived and successfully used to predict experimental data. It was demonstrated that the MID can be calculated numerically for microspheres with known statistical data. The equation relating between VER and microsphere size was further extended to accommodate a relation between MID and microsphere size but with limited accuracy for binders of low starch content. An alternative empirical linear equation for the relation between MID and microsphere size

[1] Corresponding author

was proposed for wider applications. A simple method for estimation of syntactic foam density prior to completion of manufacture was suggested. Shrinkage after molding of syntactic foam was discussed in relation with different stages such as slurry, dough and solid. A two-step manufacturing process viz molding and then forming was suggested for syntactic foam dimensional control.

Keywords: Syntactic foam, Manufacturing, Buoyancy, Starch, Gelatinization, Molding, Minimum inter-microsphere distance, Hollow microsphere, Analytical modelling, Numerical analysis, Slurry, Dough, Volume expansion of bulk microspheres, Shrinkage, Forming

1. Introduction

Syntactic foams are made of pre-formed hollow microspheres and binder(1). They can be used in various structural components including sandwich composites(2,3) and in areas where low densities are required e.g. undersea/marine equipment for deep ocean current-metering, anti-submarine warfare(4-8) and others(9). Their other uses include products in aerospace and automotive industries(9). The densities of syntactic foams in the past, however, have been relatively high compared to the traditional expandable foams, limiting their applications.

A wide range of different types of syntactic foams can be made by selecting different materials and consolidating techniques. The consolidating techniques include coating microspheres(10). rotational molding(11), extrusion(12,13) and ones that use inorganic binder solution and firing(14), dry resin powder for sintering(15-18), compaction(19,20), liquid resin as binder(21) for in situ reaction injection molding, and buoyancy(1,22,23). The last method (buoyancy) has recently been demonstrated to be capable of control of a wide range of binder contents at low costs, widening

applicability of syntactic foams. Also it allows us to use starch as binder for manufacturing syntactic foams.

In this paper, the manufacturing method based on the 'buoyancy principle' is employed for manufacturing syntactic foams consisting of ceramic hollow microspheres and starch. Starch has some advantages over other binders such as epoxies, phenolics, etc in some potential applications such as building interior sandwich panels. It is readily available, environmentally friendly, and an inexpensive renewable polymeric binder. However, it is dimensionally unstable during manufacturing, limiting its applicability. For example, gelatinized starch binder shrinks significantly when it dries. A main purpose in the present work was to investigate relationships between various manufacturing parameters, which would be useful for design of manufacturing facilities and for manufacturing syntactic foams with dimensional control.

2. Constituent materials for syntactic foams

2.1. Hollow Microspheres

Ceramic hollow microspheres (composed of silica 55-60%, alumina 36-40%, iron oxide 0.4-0.5% and titanium dioxide 1.4-1.6%) supplied by Envirospheres Pty Ltd, Australia were used. Four different size groups (or commercial grades), SL75, SL150, SL300 and SL500, were employed. Scanning electron microscope (SEM) images of hollow microspheres are given in **Figure 1**.

Microsphere sizes were measured using a Malvern 2600C laser particle size analyser and were found to be of approximately Gaussian distribution as shown in **Figure 2**. Particle densities and bulk densities of the four hollow microsphere groups were also measured using a Beckman Air Comparison

Pycnometer (Model 930, Fullerton, California) and a measuring cylinder (capacity 250cc) respectively. Three hundred taps were conducted for each bulk density measurement. An average of five measurements was taken for each size group and all values are listed in **Table 1**.

2.2. Starch as binder

Potato starch (Tung Chun Soy & Canning Company, Hong Kong) was used as binder for hollow microspheres. Particle density of the potato starch was measured using a Beckman Air Comparison Pycnometer (Model 930) and an average of three measurements was found to be 1.50g/cc. Bulk density was also measured using a measuring cylinder with a tapping device (300 taps were conducted) and an average of five measurements was found to be 0.85g/cc. **Figure 3** shows SEM images of starch granules employed. A gelatinisation temperature range for starch was measured to be 64-69ºC.

Viscosities of binder consisting of various contents of gelatinised starch in water were measured at 25°C using a Cannon-Fenske Routine viscometer (for low viscosities) and a Brookfield Synchro-Lectric viscometer (LVF 18705) (for high viscosities). Results are shown in **Figure 4**.

3. The buoyancy method for manufacturing syntactic foams

The basic principles for manufacturing of syntactic foams containing starch as binder are based on buoyancy of hollow microspheres in aqueous starch binder. The starch binder can be diluted for the purpose of controlling binder content in syntactic foam. When microspheres are dispersed in binder in a mixing container as a result of stirring/tumbling, the mixing container is left until microspheres float to the surface and starch settles down, forming three phases i.e. top phase consisting of microspheres

and binder, middle phase of water, and bottom phase of starch/microspheres and water. The top phase is to be used for molding. Gelatinisation of starch in the mixture can be conducted in two different ways of timing. One is prior to the addition of hollow microspheres to water-starch mixture and the other after molding, which will be referred to as pre- and post-mold gelatinisations respectively. In this work, pre-mold gelatinisation was employed. More details are available in references(22,23).

4. Phase separation measurement of mixture

Measuring cylinders (500cc, 50mm in diameter) shown in **Figure 5** were used for observation of phase separation and measurements of phase volumes at a room temperature range of 17 - 20°C. A wooden lid was used on the top of each cylinder to minimise evaporation of water from the mixture. A constant volume of 400cc for binder in each cylinder was used. Phase volume was monitored every 30 minutes until a constant value in three successive readings was found and then the constant value was used for each phase volume measurement.

Measurements for phase volumes were also made prior to adding microspheres. Gelatinised starch (only two phases in this case) was found to settle down in 2 to 6 hours in binder, depending on starch content in binder. After adding microspheres to binder, phase separation (three phases in this case) took 3 to 8 hours in binder, depending on microsphere size and starch content in binder. Tumbling of mixture containing microspheres was conducted after sealing by turning each measuring cylinder upside-down and back up for 20 times manually (a plateau value for phase separation was found after 5 times turning). This way of tumbling intended to break up possible starch-rich area in binder efficiently. (It was found that a spatular/stick stirring results in a substantial difference in phase volumes compared to the current tumbling.)

5. Top phase volume calculation

5.1 Numerical calculation of minimum inter-microsphere distance

The top phase volume is always larger than the initial bulk volume of microspheres in air (IBVMS) as a result of expansion of IBVMS caused by starch binder between microspheres. A minimum inter-microsphere distance (MID) may be an indicator of the volume expansion of IBVMS when microspheres are dispersed in the top phase. (The MID is a surface-to-surface distance.) A computer program was written in MATLAB 6.5 to produce 3D models for dispersion of microspheres and to find a MID for a given volume fraction of microspheres. Microspheres with random sizes but with Gaussian distribution as measured for microspheres (See **Figure 2**) were randomly positioned in 3D space. Mean radii corresponding to experimental values, 26.72, 55.27, 89.09, and 179.73 μm were nominated for SL75, SL150, SL300, and SL500 respectively, with respective standard deviations of 7.06, 18.2, 29.95, and 58.83 μm. 3D model space size for dispersion of microspheres was varied depending on microsphere size to reduce the computer running time. Thus, a box with dimensions of 500 x 500 x 500 μm was used for SL75, a box with dimensions of 1000 x 1000 x 1000 μm for both SL150 and SL300, and a box with dimensions of 2000 x 2000 x 2000 μm for SL500.

The 3D random positions of microspheres were created by assigning random values for Cartesian coordinates for each position. Microspheres were collected until a nominated volume fraction of microspheres is reached but by rejecting ones that are closer to existing microspheres than a nominated MID. A total number of trials with microspheres for a given MID was 20,000 at which a total number of collected microspheres in a box is identical with that at $15{,}000^{th}$ microsphere. Iteration was conducted to find a MID corresponding to a volume fraction of microspheres experimentally given and was ended when

$$\frac{|\, v_{ms} \text{ from experiment} - \text{Calculated } v_{ms} \,|}{v_{ms} \text{ from experiment}} \leq 0.048 \qquad (1)$$

where v_{ms} is the volume fraction of microspheres. The collected microsphere numbers in the boxes varied depending on MID value and their ranges were 22 to 127 for SL75, 43 to 121 for 150, 20 to 31 for SL300, and 20 to 43 for SL500.

5.2 Idealised mono-sized particle dispersion models

Idealised mono-sized particle dispersion models i.e. simple cubic (SC) unit cell, face centred cubic (FCC) unit cell, and body centred cubic (BCC) unit cell are shown in **Figure 6** for derivation of volume expansion rate (VER) of bulk microspheres in the top phase being defined as (top phase volume) / IBVMS.

The VER based on the three models (independent of model type) was derived to be

$$VER = \left(1 + \frac{d_e}{2r + d_0}\right)^3, \qquad (2)$$

where r is the radius of microsphere, d_0 is the initial *MID*, and (d_0+d_e) is the *MID* after expansion. For a practical microsphere dispersion in the top phase, equivalent values for d_0 and d_e can be found. The d_0, when d_e = 0, in Equation (2) was calculated for each microsphere size group using the packing

factor (= microsphere bulk density / microsphere particle density) of bulk microspheres for a given mean radius of microspheres and given in **Table 2**.

6. Shrinkage measurement and characteristics after molding

Rectangular open molds made of aluminium strip with cavity dimensions 110 x 30 x 16mm were used for specimens for shrinkage measurement. Each mold was placed on an aluminium plate covered with paper prior to molding. A releasing agent (Release Paste 7, Dow Corning) was used for the molds. Molded specimens were dried in an oven at 80°C. Also, different stages for molded specimen dependant upon dryness were monitored. The first stage was slurry, the second stage dough and the third stage solid. The second stage was of reversible shape whereas the third was of irreversible shape. Two specimens were used for each set of measurements.

7. Results and discussion

Volume fraction of bottom phase consisting of starch sediment without using microspheres (SSWMS) (only two phases in this case formed) measured in a measuring cylinder versus initial granule starch content prior to gelatinization is shown in **Figure 7**. As expected, the gelatinised starch sediment is approximately proportional to starch content as the high correlation coefficient of 0.988 with a forced intercept at zero indicates. The slope (= 42) may be used to quantify starch expansion as a result of gelatinisation swelling.

It is noted that volume fraction of bottom phase of gelatinised starch approaches a value of 1 (**Figure 7**) at a volume fraction of initial granule starch of about 0.022 corresponding to a viscosity of 715 centipoise (see **Figure 4**) at which viscosity increases rapidly. Also, it was experienced that, when

starch content is higher than 0.022, molding of mixture consisting of microspheres and binder was difficult. Thus, the point (a volume fraction of 1), at which no phase separation would occur, appears to be a critical point that may be used as the practical limit of workability range for molding.

VER of IBVMS in the top phase after tumbling/stirring is plotted in **Figure 8** as a function of starch content in binder. It is surprisingly high particularly for small sized microspheres (SL75) to be over 30 and is also high for high starch content and low IBVMS. The effect of IBVMS on the expansion rate seems to be due to the buoyant force because the smaller the IBVMS, the lower the buoyant force, giving smaller squeezing force and hence larger inter-microsphere distances. Also, it is a truism that the volume expansion is caused by distance increase between microspheres. Once microspheres are wetted with binder, their distances between microspheres would be affected by various factors such as starch content, IBVMS, etc. Surfaces of top phases of SL75 and SL500 were viewed under an optical microscope as shown in **Figure 9**. Some distances between microspheres are vaguely seen in SL75 and are obvious in SL500. It was assumed that a MID exists in the top phase for a given manufacturing condition. Also, the top phase can be assumed as being formed through random positioning of microspheres after the tumbling/stirring. Numerical calculations were conducted on the basis of these two assumptions as detailed in section **5** and some examples of 3D numerical models used are given in **Figure 10**. The experimental VER versus numerically calculated MID (= d_0+d_e) is shown in **Figure 11** with theoretical curves generated according to Equation (2). The theoretical curves based on BCC and FCC models appear to be in a good agreement with data. Meanwhile, SC model appears to be in a relatively poor agreement with data compared to the other models and has unrealistic values for d_0 being negative as listed in **Table 2**. The predictions based on BCC and FCC would be useful for practical design of mixing containers for different microsphere sizes and eventually for optimization of manufacturing system. Furthermore, a relationship between MID (or

VER) and microsphere size is also useful. An approximate relationship for $d_0 << d_e$ (or $d_0 \approx 0$) can be found from Equation (2) as

$$MID = 2(VER^{1/3} - 1)r \quad (3)$$

where r is the mean radius of microsphere size group. Correlation coefficients (between MID and r) found for Equation (3) are listed in **Table 3**. The correlation coefficient is acceptably high for high starch content in binder and high IBVMS although it is generally poor. Alternatively, another relationship was empirically found for the whole range of data collected in this work for a given starch content and IBVMS:

$$MID = a + br \quad (4)$$

where a and b are constants. All the values in Equation (4) found are listed with correlation coefficients in **Table 3**. A range of correlation coefficients was found to be 0.961 - 0.998, supporting the validity of Equation (4). Some examples showing the linear relationship between *MID* and r are given in **Figure 12** for different starch contents but a constant initial microsphere bulk volume of 20cc.

Now, the top phase consists of microspheres and binder. The binder trapped between microspheres in top phase further consists of starch and water. Starch concentration in binder trapped in the top phase (BTTP) can be found using a volume rate (VR) defined as

$$\mathrm{VR} = \frac{\text{Volume of SSTTP}}{\text{Volume of BTTP}} \quad (5)$$

where SSTTP is the starch sediment increment when no micropspheres are used and is illustrated in relation with SSWMS in **Figure 13**. VR values are given in **Table 4**. Each mean value of VR was obtained from 5 different IBVMS's (10cc, 15cc, 20cc, 25cc, and 30cc) for a given microsphere size group and starch content in binder. VR's are seen to be not much dependant on IBVMS as the low standard deviations indicate. Also, VR appears to decrease as the volume fraction of SSWMS in binder decreases, indicating that starch concentration in BTTP decreases with decreasing viscosity of binder.

The quantities of SSTTP and IBVMS would be useful for foam density estimation prior to manufacturing if a final volume of foam would be equal to IBVMS. There is some difference, though, between the final volume of foam and IBVMS as listed in **Table 5** with other measurements for manufactured syntactic foams. It is found that (a) volume ratio of foam/bulk microspheres is in a range of 1.1 -1.3 and (b) the larger the microsphere size the lower the ratio. Still some useful estimation for the foam density but with some error range appears to be achievable.

Shrinkage of microsphere-binder mixture for SL150 after molding, measured in percentage of initial volume for different mass ratios of water/starch in binder (50/1, 70/1 and 90/1) is given in **Figure 14 (a)** as a function of drying time. Density change due to drying for the same molded mixture is also given in **Figure 14 (b)** with different stages being defined earlier for dough and solid. Two different stages are seen in **Figure 14 (a)** i.e. shrinkage rapidly occurs at an early stage until about 120 min for all water/starch mass ratios and then reaches a plateau value at a later stage - this was found for all other microsphere size groups also. The transition between the two stages of shrinkage (**Figure 14 (a)**) corresponds with a transition from dough to solid shown in **Figure 14 (b)**. It can be deduced that positions of microspheres in a molded mixture stabilise at the transition (in **Figure 14(a)**) after the

large shrinkage, making water evaporation difficult as a result of reduction of inter-microsphere distances. Subsequently, the molded mixture goes into the stage of solid at which forming is difficult. In practical manufacturing, a two-step process viz molding first and then forming at a point prior to the transition between dough and solid would be suggested for foam dimensional control.

Some example images of polished cross sections for manufactured syntactic foams after embedding in an epoxy are shown in **Figure 15**. Voids between microspheres are not identifiable due to preparation technique but other quantities as given in **Table 5** are comparable with the images.

8. Conclusions

- Various parameters for syntactic foam manufacture based on the 'buoyancy method' have been studied.

- Minimum inter-microsphere distance (MID) concept for volume expansion of bulk microspheres caused by gelatinized starch is introduced.

- MID has been numerically calculated for various volume expansion rates of bulk microspheres.

- An equation (Equation (2)) based on unit cell models with MID concept for a relation between VER and microsphere size is derived and successfully used to predict experimental data.

- The Equation (2) is further extended to accommodate a relation between MID and microsphere size but with some limited accuracy for binders of low starch content. An

alternative empirical linear equation (Equation (4)) is proposed for wider applications for the relation between MID and microsphere size.

- A simple method for estimation of syntactic foam density prior to completion of manufacture is suggested

- A two-step manufacturing process viz molding and then forming is suggested for syntactic foam dimensional control.

Acknowledgement

The authors gratefully acknowledge the International Postgraduate Research Scholarship (IPRS) and the University of Newcastle Research Scholarship (UNRS) provided for Md M. Islam, and the financial support from The University of Newcastle Research Associates (TUNRA).

References

1. Kim H.S.; Plubrai P. Manufacturing and failure mechanisms of syntactic foam under compression. Composites Part A: Applied Science and Manufacturing 2004, 35(9), 1009-15.

2. Jize N.N.; Hiel C.; Ishai O. Mechanical Performance of composite sandwich beams with syntactic foam cores. In Deo RB and Saff CR , Eds. ASTM STP 1274, 1996. p.125-138.

3. English L.K. Lighter weight and lower cost with foam-core composites. Materials Engineering 1987, 4, 51-54.

4. Jackson D.; Clay P. Syntactic foam sphere improves oceanographic mooring performance. Sea Technology Sept 1983, 24, 29-31.

5. Harruff P.W.; Sandman B.E. In Carbon/epoxy composite structures for underwater pressure hull applications. Proceedings of 28th National SAMPE Symposium, Anaheim, CA, April 12-14, 1983. p. 40-49.

6. Watkins L. In Syntactic foam buoyancy for production risers. Proceedings of the Seventh International Conference on Offshore Mechanical and Artic Engineering, Houston, Texas, Feb 7-12, 1988. p.403-410.

7. Seamark, M.J. Use of syntactic foam for subsea buoyancy. Cellular Polymers 1991, 10(4), 308-321.

8. Hinves J.B.; Douglas C.D. The development of a hybrid advanced composite-syntactic foam structural component for use in undersea vehicles. IEEE 1993, p.III-468 – 472.

9. Young K.S. Value-adding syntactic foams gain in composites applications. Modern Plastics April 1985, p.92-97.

10. Narkis M.; Gerchcovich M.; Puterman M.; Kenig S. Syntactic foams III. Three-phase materials produced from resin coated microballoons. Journal of Cellular Plastics July/August 1982, p. 230-232.

11. Narkis M.; Puterman M.; Boneh H. Rotational molding of thermosetting three-phase syntactic foams. Polymer Engineering and Science 1982, 22, 417-421.

12. Lawrence E.; Wulfsohn D.; Pyrz R.. Microstructural characterisation of a syntactic foam. Polymers and Polymer Composites 2001, 9(7), 449-457.

13. Lawrence E.; Pyrz R. Viscoelastic properties of polyethylene syntactic foam with polymer microballoons. Polymers and Polymer Composites 2001, 9(4), 227-237.

14. Verweij H.; De With G.; Veeneman D. Hollow glass microsphere composites : preparation and properties. Journal of Materials Science 1985, 20,1069-1078.

15. Narkis M.; Puterman M.; Kenig S. Syntactic foams II. Preparation, and characterization of three-phase systems. Journal of Cellular Plastics Nov/Dec 1980,326-330.

16. Puterman M.; Narkis M. Syntactic foams I. Preparation, structure and properties. Journal of Cellular Plastics July/August 1980,223-229.

17. Kenig S.; Raiter I.; Narkis M. Three-phase silicone based syntactic foams. Journal of Cellular Plastics Nov/Dec 1984, 423-429.

18. Meter C. Syntactic foam core material for composite structures, International patent classification : B29C, 65/00, B29D 9/00, B32B 3/26, 5/18.

19. Kim H.S.; Oh H.H. In Impact behaviour of syntactic foam, Proceedings of the first ACUN International Composites Meeting on Composites : Innovation and Structural Applications. Sydney, 23-25 February, 1999. p.83-86.

20. Kim H.S.; Oh H.H. Manufacturing and Impact Behavior of Syntactic Foam. Journal of Applied Polymer Science 2000, 76, 1324-1328.

21. te Nijenhuis K.; Addink R.; van der Vegt A.K. A study on composites of nylon-6 with hollow glass microspheres. Polymer Bulletin 1989, 2, 467-474.

22. Kim H.S. Syntactic foam, International Publication Number: WO 03/074598 A1, International Publication Date: 12 Sept 2003.

23. Kim H.S. Method of forming syntactic foams, International Publication Number: WO 2006/005119 A1, International Publication Date: 19 January 2006.

Table 1 Particle and bulk densities of hollow microspheres employed**.**

Hollow microspheres	Particle density (g/cc)	Bulk density (g/cc)
SL75	0.68	0.39
SL150	0.73	0.42
SL300	0.80	0.43
SL500	0.89	0.36

Table 2 Packing factors and d_0 values of bulk microspheres for different microsphere size groups.

Hollow microspheres	Packing factor of bulk microspheres	d_0 for SC (μm)	d_0 for FCC(μm)	d_0 for BCC(μm)
SL75	0.57	-1.49	4.87	3.24
SL150	0.58	-3.40	9.72	6.37
SL300	0.54	-1.82	19.77	14.25
SL500	0.40	33.76	81.91	69.59

Table 3 Correlation coefficients for Equation (3) and values in Equation (4), $MID = a + br$, with correlation coefficients.

Initial bulk Volume of microspheres (IBVMS) (cc)	Starch volume fraction in binder	Correlation coefficient for Eq (3)	*a*	*b*	Correlation coefficient for Eq (4)
10	0.0217	0.889	79.	1.69	0.993
10	0.0132	0.179	99	0.93	0.985
10	0.0094	0.206	90	0.88	0.990
10	0.0074	0.489	80	0.88	0.990
10	0.006	0.466	75	0.81	0.991
15	0.0217	0.933	63	1.76	0.992
15	0.0132	0.469	90	0.97	0.979
15	0.0094	0.774	66	1.01	0.994
15	0.0074	0.791	61	0.96	0.989
15	0.006	0.791	57	0.91	0.988
20	0.0217	0.959	50	1.84	0.992
20	0.0132	0.722	74	1.06	0.967
20	0.0094	0.830	59	1.04	0.981
20	0.0074	0.896	46	1.06	0.985
20	0.006	0.912	40	1.01	0.985
25	0.0217	0.981	35	1.86	0.997
25	0.0132	0.809	61	1.05	0.973
25	0.0094	0.872	47	0.98	0.981
25	0.0074	0.895	42	0.98	0.981
25	0.006	0.922	33	0.98	0.974
30	0.0217	0.979	33	1.60	0.998
30	0.0132	0.830	52	0.97	0.964
30	0.0094	0.919	35	1.02	0.972
30	0.0074	0.920	32	0.99	0.967
30	0.006	0.921	29	0.96	0.961

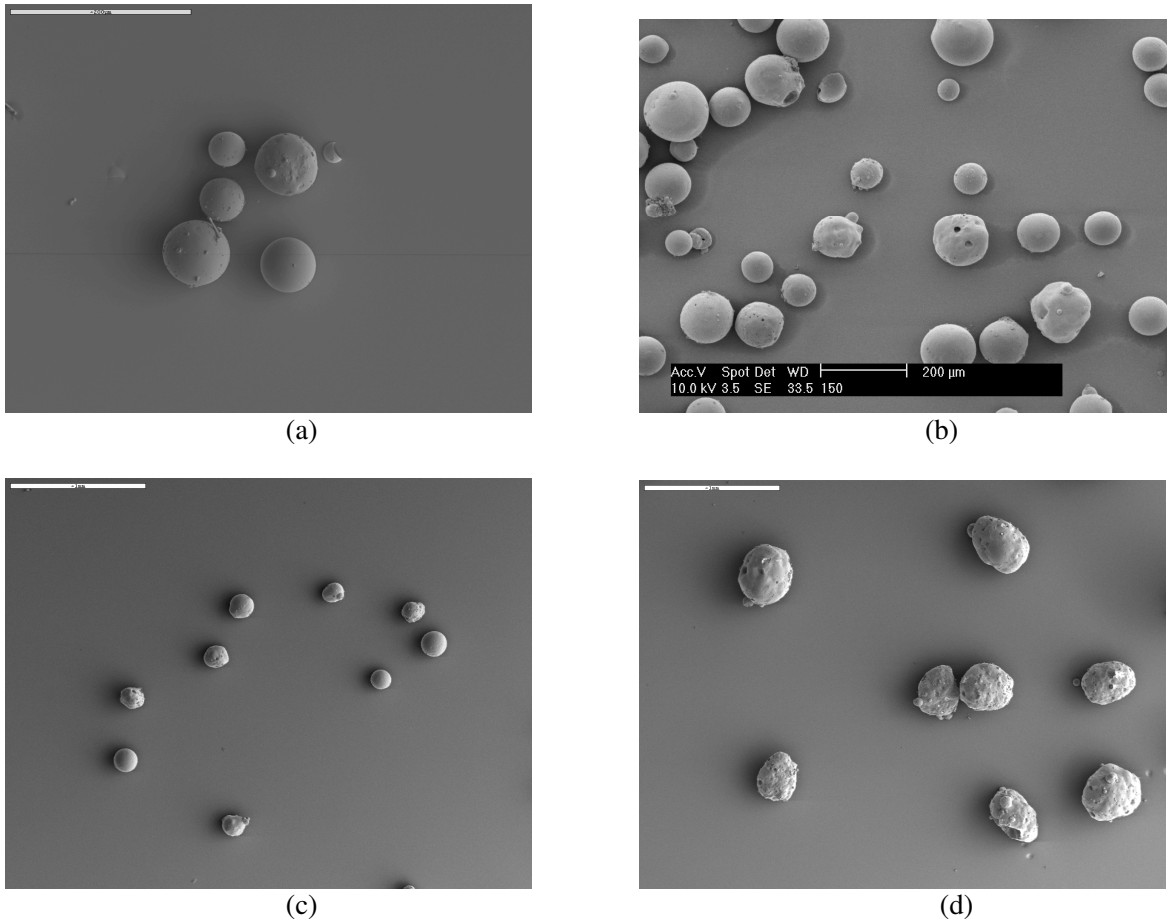

(a) (b)

(c) (d)

Figure 1 SEM images of hollow microspheres: (a) SL75 (the scale bar represents 200 µm); (b) SL150 (the scale bar represents 200 µm); (c) SL300 (the scale bar represents 1 mm); and (d) SL500 (the scale bar represents 1 mm).

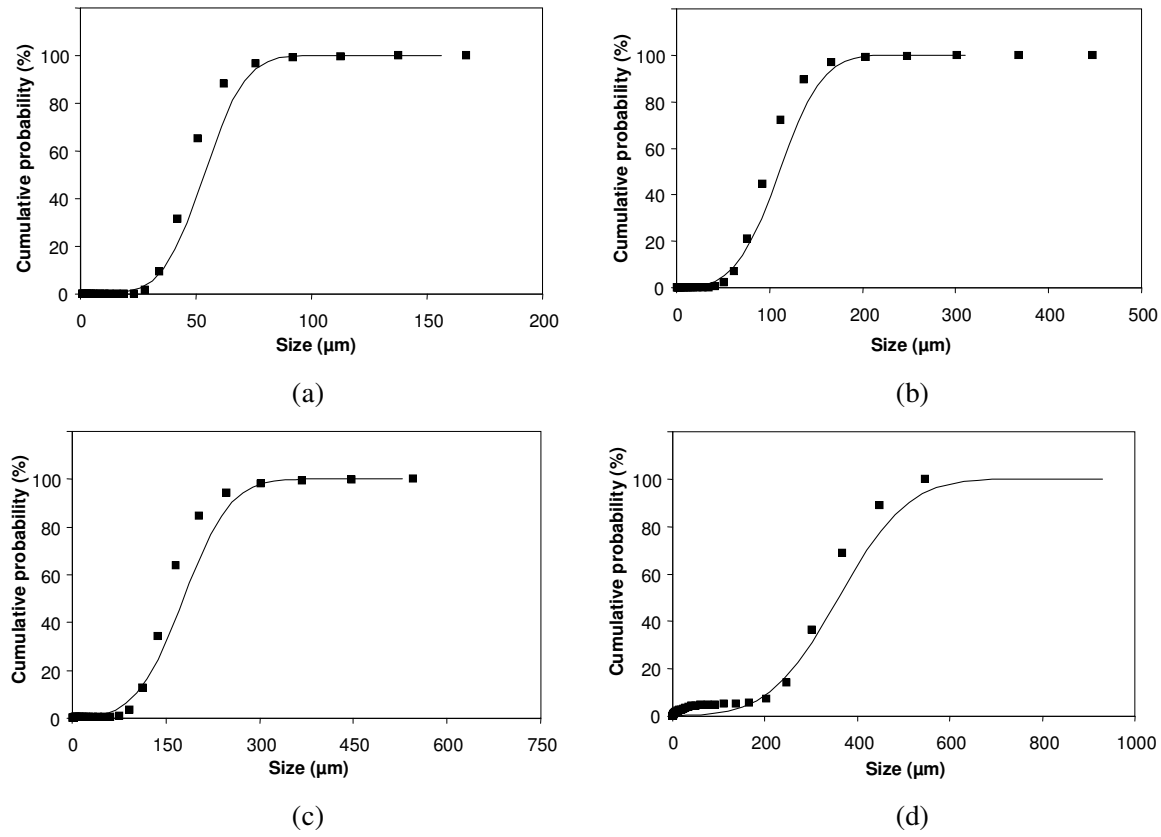

Figure 2 Size distributions of different hollow microsphere size groups with the cumulative Gaussian distribution curves: (a) SL75; (b) SL150; (c) SL300; and (d) SL500.

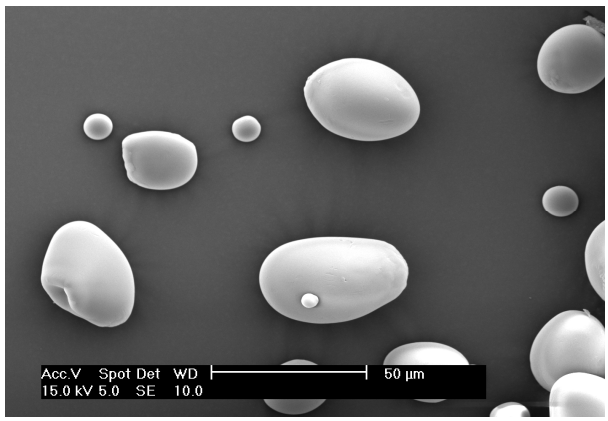

Figure 3 SEM image of potato starch granules prior to gelatinisation.

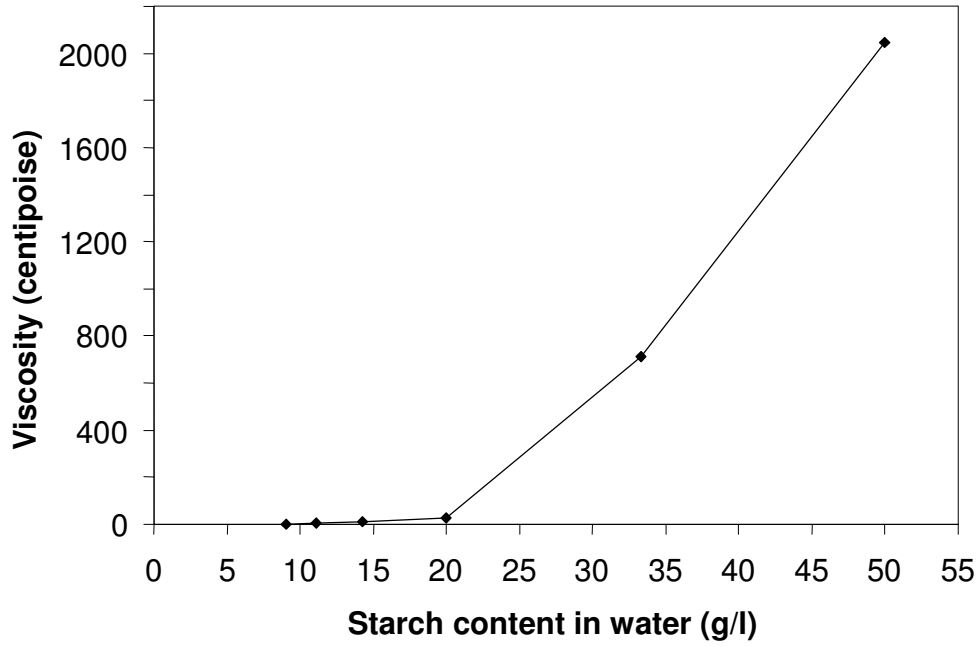

Figure 4 Viscosity of binder consisting of gelatinised starch and water as a function of starch content in water.

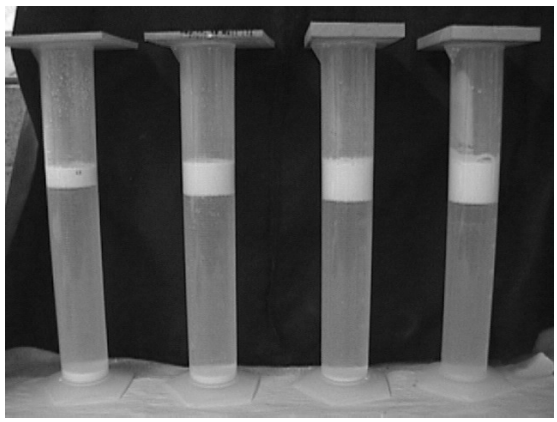

Figure 5 Phase separation experiment with SL500, SL300, SL150 and SL75 (from left to right). Three phases are formed after stirring in each measuring cylinder.

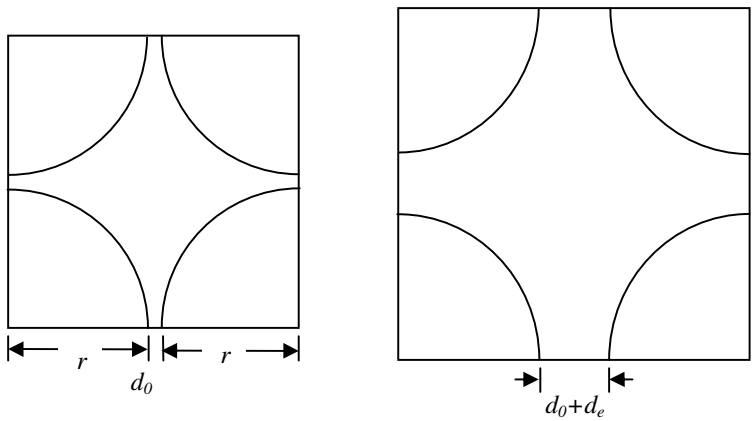

(Before) (After)

(a)

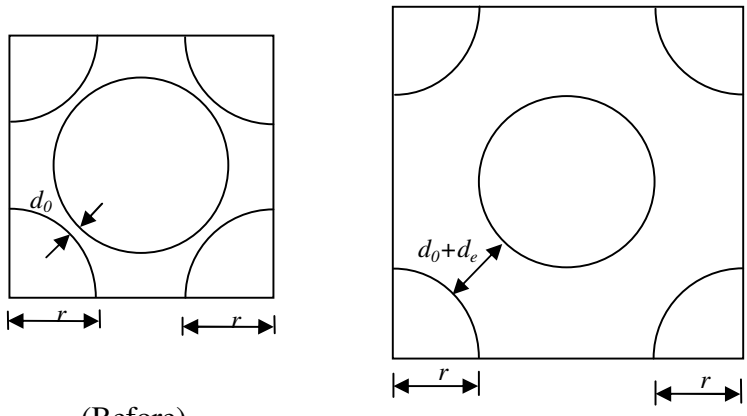

(Before) (After)

(b)

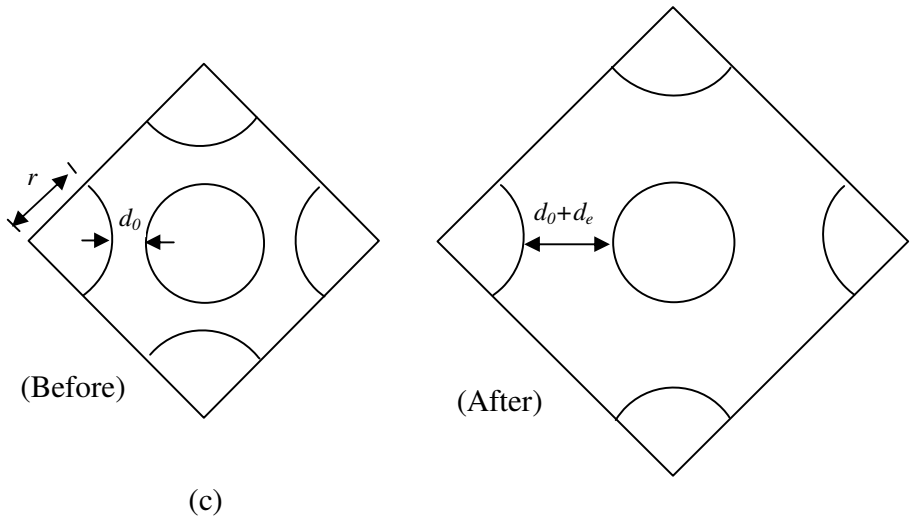

(c)

Figure 6 Mono-sized microsphere models before and after expansion of bulk microspheres: (a) front view of simple cubic (SC) unit cell; (b) front view of face centred cubic (FCC) unit cell; and (c) diagonal cross section view of body centred cubic (BCC) unit cell.

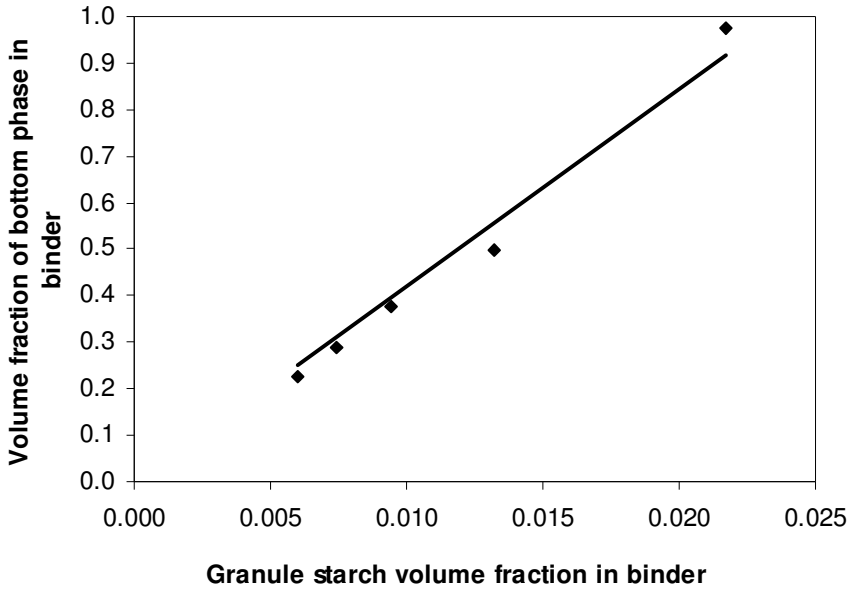

Figure 7 Volume fraction of gelatinised starch sediment (bottom phase) measured in a cylinder without microspheres versus initial granule starch volume fraction. Correlation coefficient of the best fit line with a forced intercept at zero is 0.988.

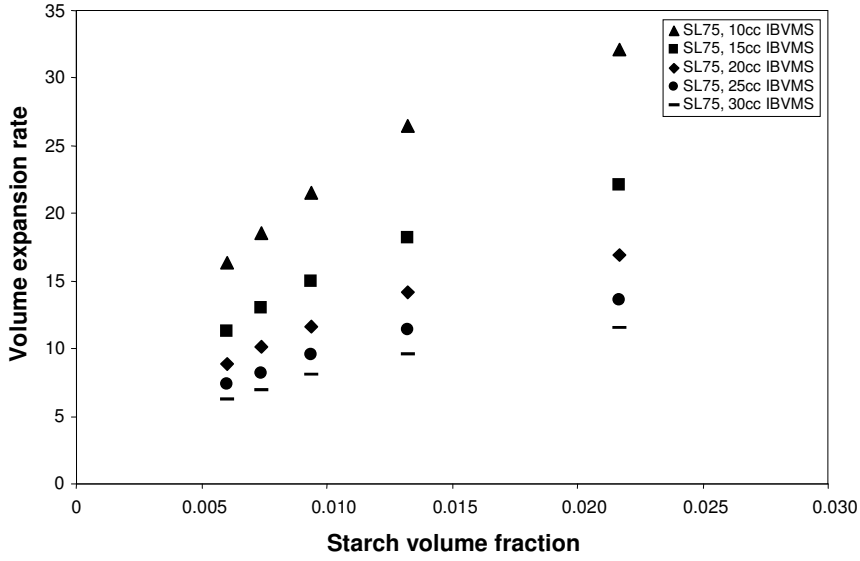
SL75, 10cc IBVMS
SL75, 15cc IBVMS
SL75, 20cc IBVMS
SL75, 25cc IBVMS
SL75, 30cc IBVMS
Volume expansion rate
Starch volume fraction
0
5
10
15
20
25
30
35
0
0.005
0.010
0.015
0.020
0.025
0.030

(a)

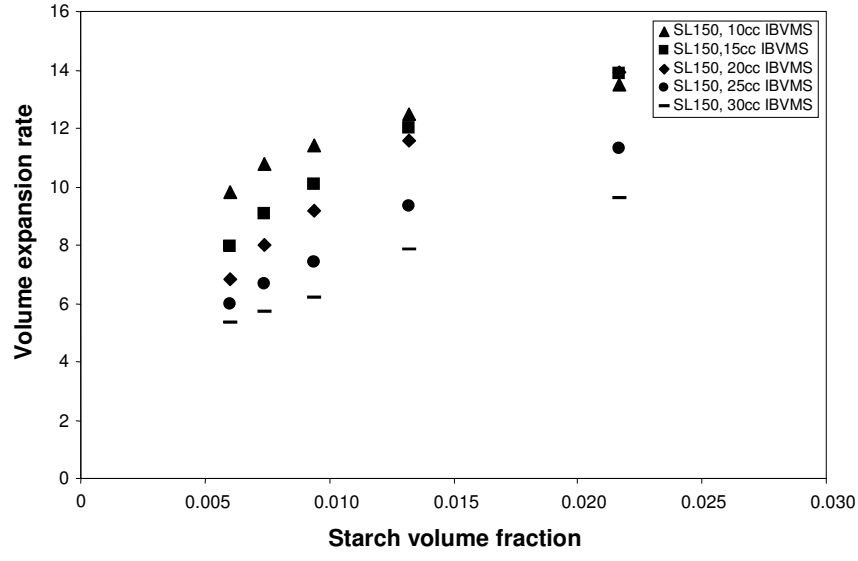
SL150, 10cc IBVMS
SL150,15cc IBVMS
SL150, 20cc IBVMS
SL150, 25cc IBVMS
SL150, 30cc IBVMS
Volume expansion rate
Starch volume fraction
0
2
4
6
8
10
12
14
16
0
0.005
0.010
0.015
0.020
0.025
0.030

(b)

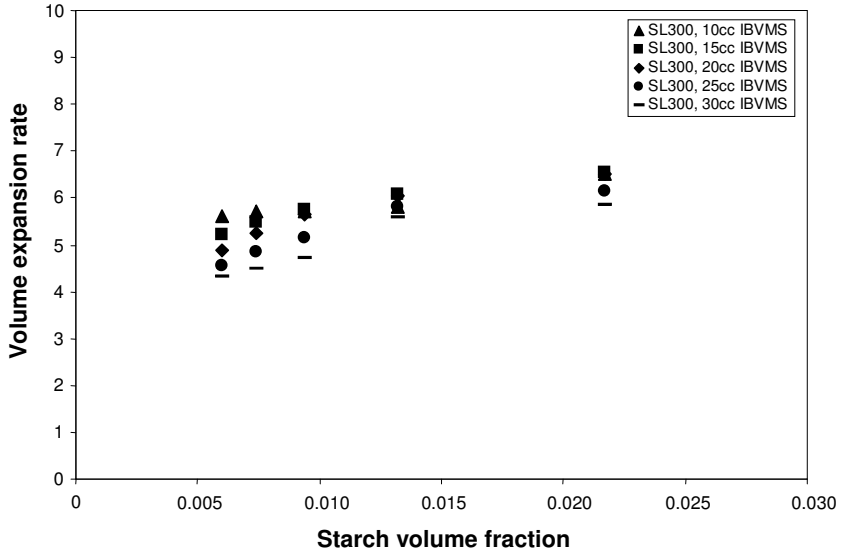

(c)

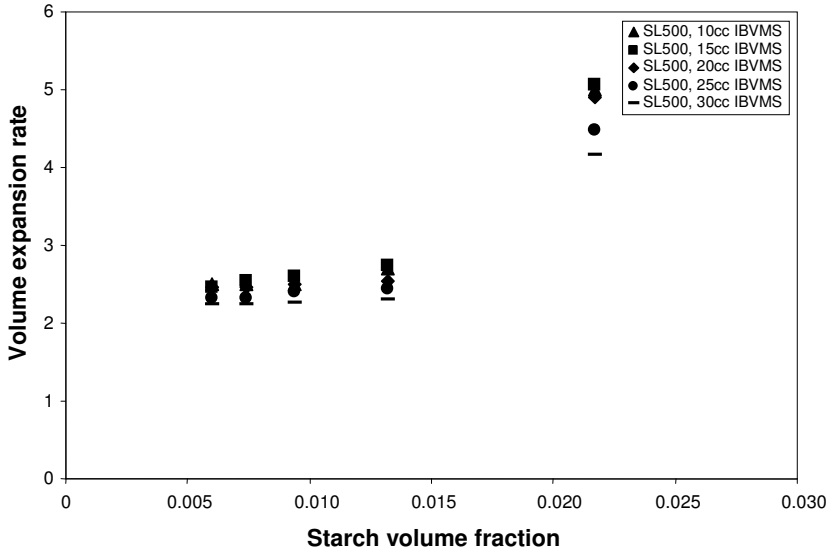

(d)

Figure 8 Volume expansion rate (VER) (= top phase volume / IBVMS) after tumbling/stirring as a function of initial granule starch volume fraction in binder: (a) SL75, (b) SL150, (c) SL300, and (d) SL500.

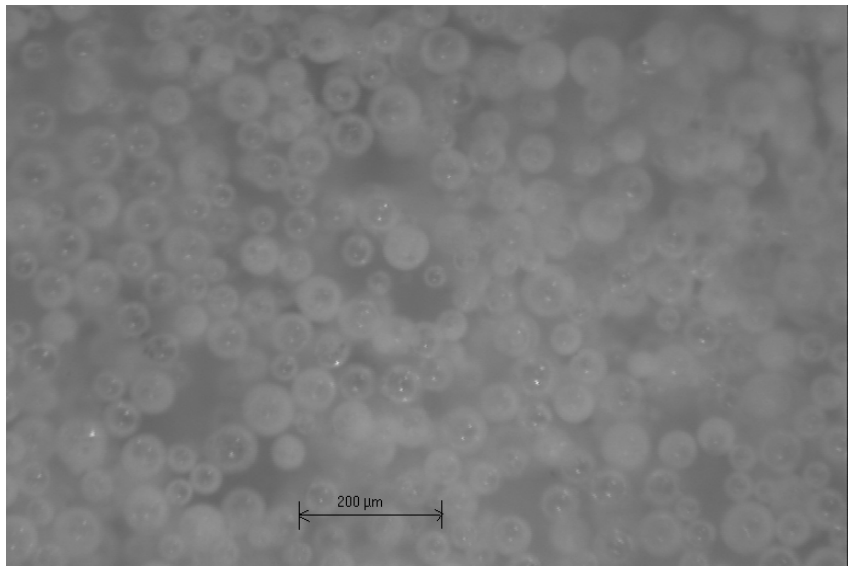

(a)

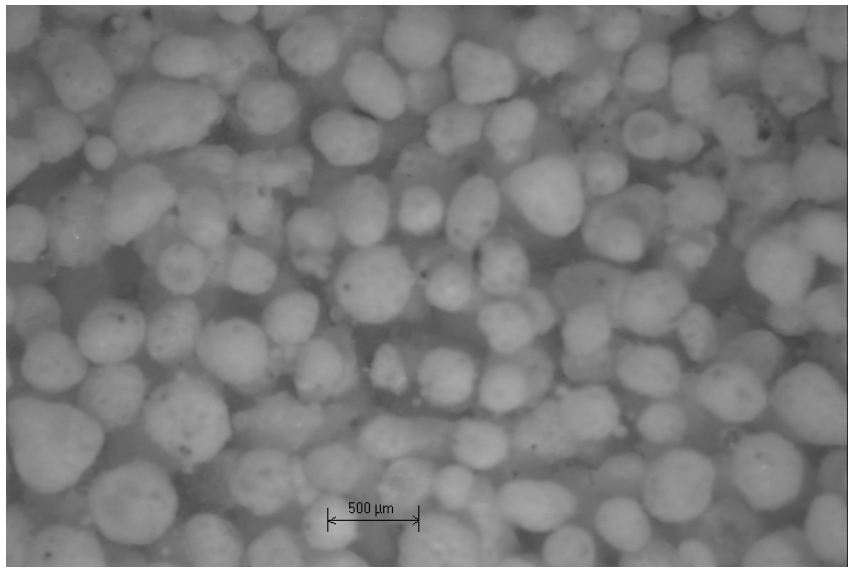

(b)

Figure 9 Surface images of the top phase consisting of gelatinised starch as binder and microspheres for a mass ratio of water/starch of 70/1 (or a volume fraction of granule starch in binder of 0.0094): (a) SL75; and (b) SL500.

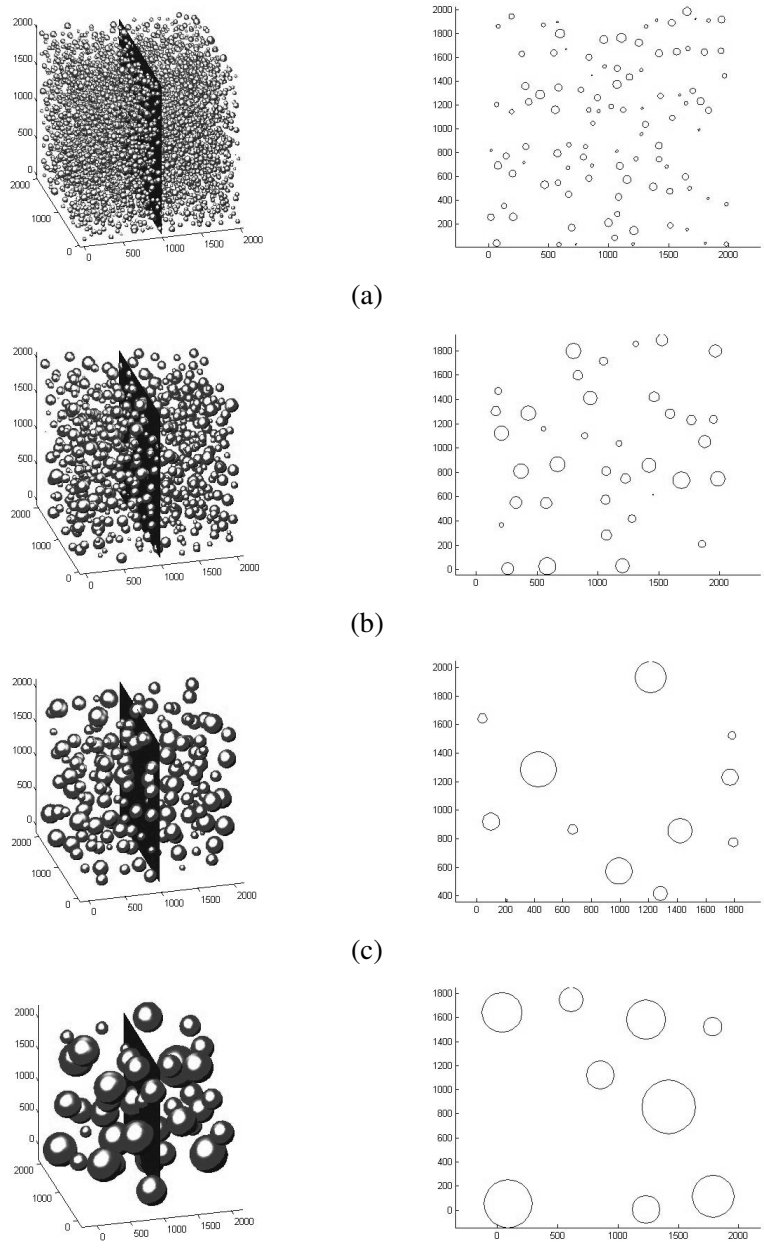

Figure 10 Some examples of 3D models with cross sections used for a manufacturing condition with an initial microsphere bulk volume of 30cc and a water/starch mass ratio of 110/1: (a) SL75, volume fraction of microspheres = 0.09, MID = 40 μm; (b) SL150, volume fraction of microspheres = 0.1, MID = 80 μm; (c) SL300, volume fraction of microspheres = 0.12, MID = 140 μm; and (d) SL500, volume fraction of microspheres = 0.18, MID = 190 μm. All scale units for the images are in μm.

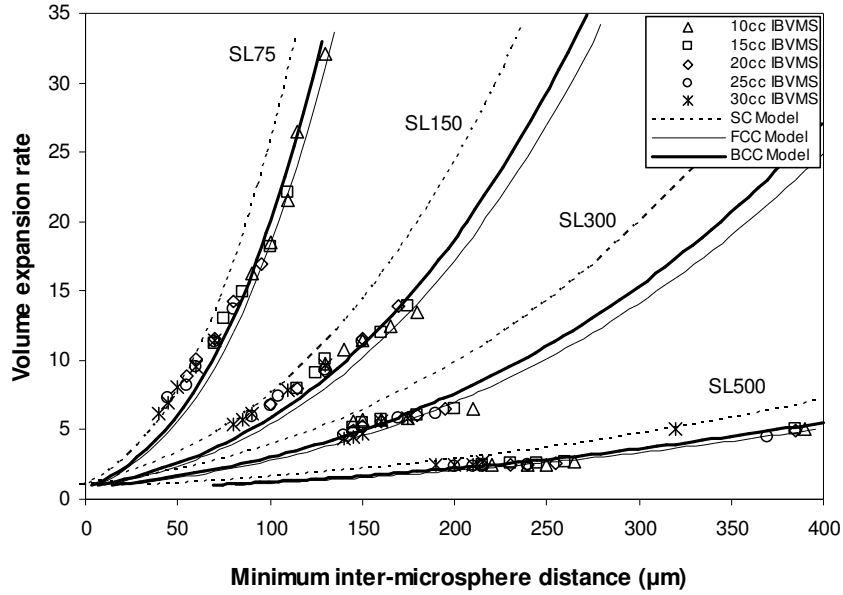

Figure 11 Experimental volume expansion rate (VER) versus numerically calculated minimum inter-microsphere distances (MID = d_0+d_e) in comparison with theoretical curves generated according to Equation (2).

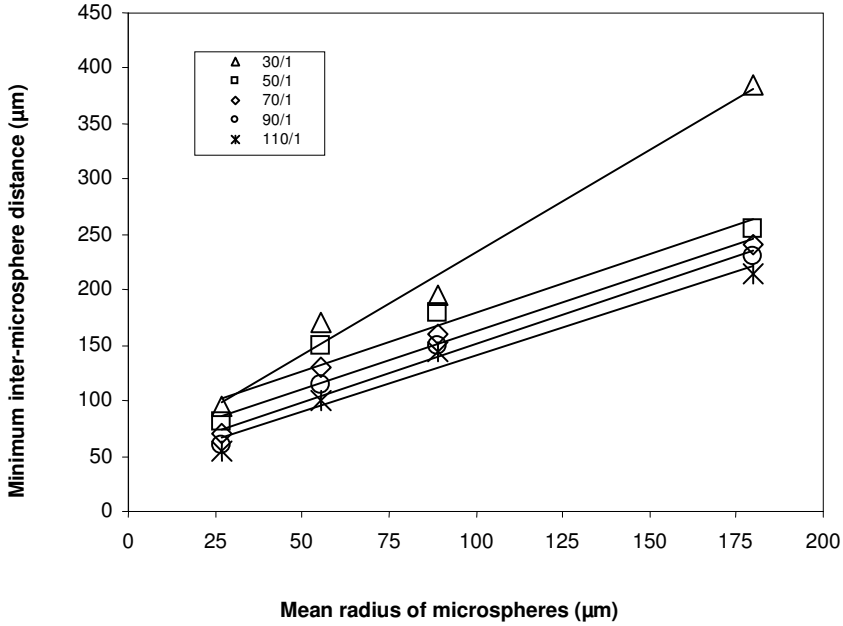

Figure 12 Some examples of linear relationship between MID and mean radius of microspheres for various mass ratios of water to starch but a constant initial microsphere bulk volume of 20cc.

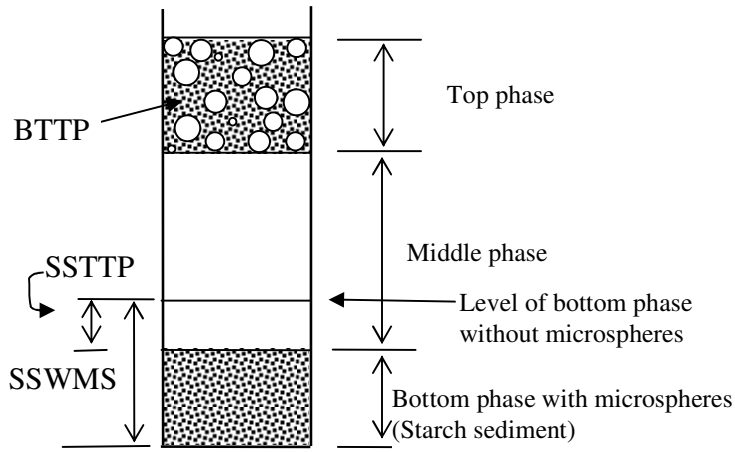

Figure 13 Schematic of various components after phase separations with/without microspheres in mixture. The 'level of bottom phase without microspheres' is for only two phases.

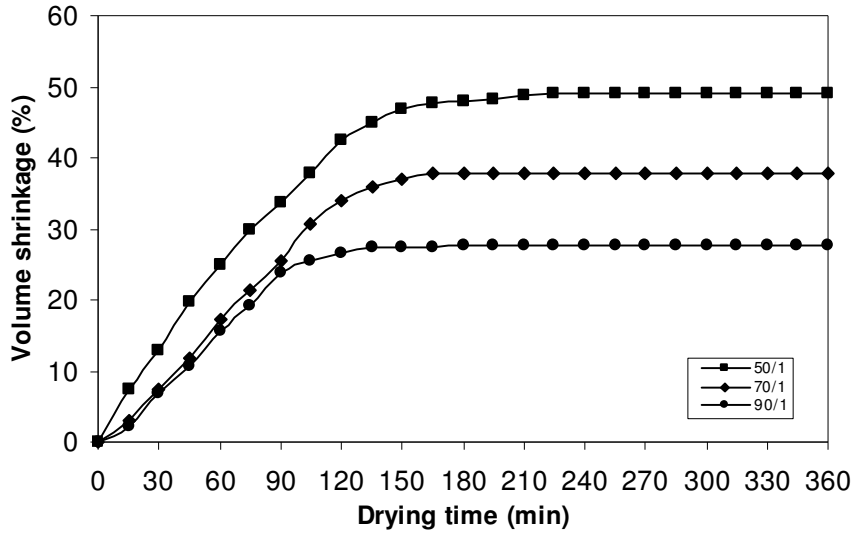

(a)

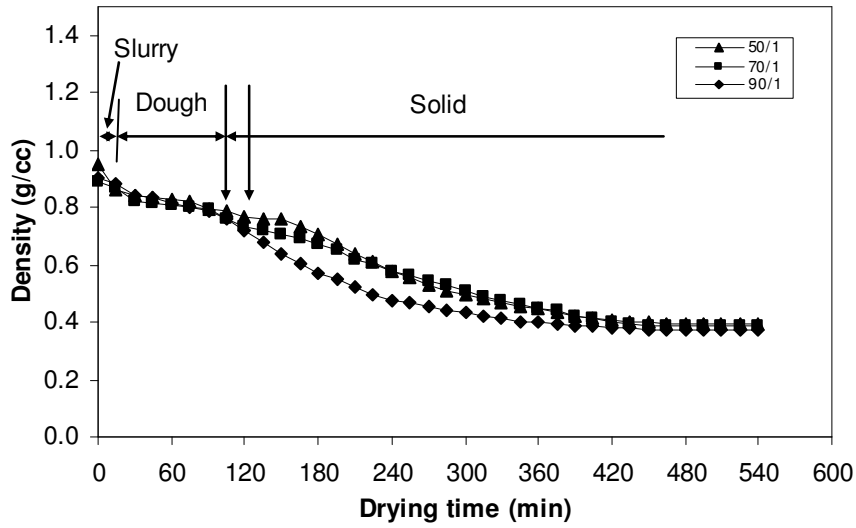

(b)

Figure 14 Shrinkage and density measurements for SL150 after molding for mass ratios of water/starch in binder – 50/1, 70/1 and 90/1: (a) shrinkage of microsphere-binder mixture in percentage of initial volume versus drying time; and (b) density of the microsphere-binder mixture versus drying time. The double arrows between dough and solid in '(b)' are to indicate a range affected by water/starch ratio – the higher starch content the longer dry time.

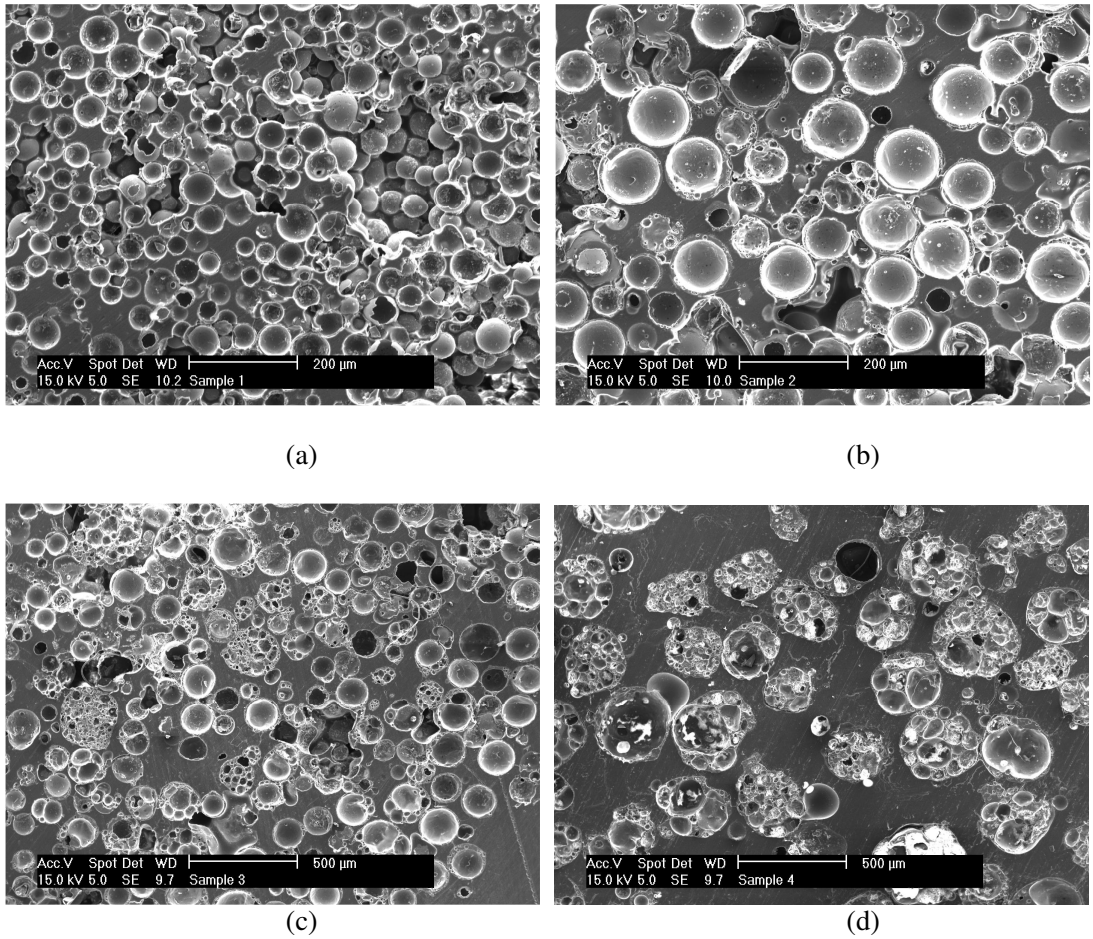

Figure 15 SEM images of the polished cross-sections of syntactic foams made of: (a) SL75; (b) SL150; (c) SL300; and (d) SL500 for a water/starch mass ratio of 70/1 in binder. Samples were prepared by embedding in an epoxy.